

On the Convergence of Gossip Learning in the Presence of Node Inaccessibility

Tian Liu^{†1}, Yue Cui^{†2}, Xueyang Hu², Yecheng Xu^{*3}, Bo Liu⁴

¹Research Institute of Intelligent Networks, Zhejiang Laboratory, Hangzhou, China

²Department of Computer Science and Software Engineering, Auburn University, Auburn, USA

³Institute of Rural Development, Zhejiang Academy of Agricultural Sciences, Hangzhou, China

⁴DBAPPSecurity Co., Ltd., Hangzhou, China

tianliu@zhejianglab.com, yuecui@auburn.edu, xueyang.hu@auburn.edu, xyc2022@zaas.ac.cn, bo.liu@dbappsecurity.com.cn

Abstract—Gossip learning (GL), as a decentralized alternative to federated learning (FL), is more suitable for resource-constrained wireless networks, such as FANETs that are formed by unmanned aerial vehicles (UAVs). GL can significantly enhance the efficiency and extend the battery life of UAV networks. Despite the advantages, the performance of GL is strongly affected by data distribution, communication speed, and network connectivity. However, how these factors influence the GL convergence is still unclear. Existing work studied the convergence of GL based on a virtual quantity for the sake of convenience, which fail to reflect the real state of the network when some nodes are inaccessible. In this paper, we formulate and investigate the impact of inaccessible nodes to GL under a dynamic network topology. We first decompose the weight divergence by whether the node is accessible or not. Then, we investigate the GL convergence under the dynamic of node accessibility and theoretically provide how the number of inaccessible nodes, data non-i.i.d.-ness, and duration of inaccessibility affect the convergence. Extensive experiments are carried out in practical settings to comprehensively verify the correctness of our theoretical findings.

Index Terms—gossip protocol, federated learning, decentralized learning, peer-to-peer system, ad-hoc network, network consensus

I. INTRODUCTION

Federated learning (FL), as a collaborative learning method, has thrived in many areas, but the need of a central server hinders its applications in wireless resource-constrained scenarios. For example, agricultural unmanned aerial vehicles (UAV) play important roles in crop scouting [1], field coverage mapping [2], plant protection [3], aquaculture water quality monitoring [4], and forest regeneration [5]. By incorporating collaborative learning into UAVs, parallel monitoring tasks, such as crop health analysis and harvest prediction, can be achieved while performing regular irrigation and fertilization operations. However, energy management in UAVs is of a significant concern. Given that agricultural UAV swarms often operate in rural areas, which are far from base stations, employing FL could rapidly drain the battery of UAVs, rendering the FL approach less feasible for such applications.

Gossip Learning (GL), as a decentralized learning algorithm, is an alternative to FL. GL can overlay the Mo-

bile Ad-Hoc Network (MANET) or Flying Ad-Hoc Network (FANET), which enables decentralized training in an infrastructure-less network layout based on opportunistic physical contacts. The decentralized framework provided by GL can greatly improve the efficiency and maximize the battery life of UAVs.

GL differs from FL in how the model aggregation is performed. Specifically, the model aggregation in GL is performed in a self-organized way, in which a pair of nodes exchange model updates if and only if they are connected by a direct communication link. The advantages of GL over FL are mainly fourfold. First, more energy efficient communication protocols, such as Wi-Fi, can be used. According to the specification of DJI Agras T16, the long distance transmission protocol (OcuSync 2.0) consumes 4 times the power of 802.11x. Second, the pairwise data sharing scheme does not rely on the full network topology. This fits FANETs where the network topology changes fast, hence nodes may not have the full network topology all the time. Third, GL is robust to single point failure, latency, and collision by redundancy introduced by the pairwise data sharing. Last, GL achieves a comparable or better performance under compression compared with FL [6], [7], which is highly suitable for network configuration with low bandwidth and high latency [8].

Despite the advantages above, the performance of GL is greatly affected by data distribution, communication speed, and connectivity [9]. It has been shown that GL maintains the original convergence speed only in network with good connectivity, i.i.d. data and homogeneous communication speed, otherwise slow convergence or biased model could happen. However, the study of how each factor affects convergence is still in its infancy.

Recently, efforts have been made to study the convergence behavior of GL in networks like MANET and FANET [10]–[12]. Since gossip protocol is an opportunistic protocol, for convenience, all the aforementioned works studied the convergence of GL based on a virtual quantity, which is the average of all local models. However, the use of this virtual quantity relies on the assumption that the gossip exchange preserves the average of the network. As shown in Fig. 1, nodes may be inaccessible due to out-of-range or link loss, conducting failure in gossiping exchange. In the presence of

[†] Equal contribution.

^{*} Corresponding author.

such nodes, the virtual average does not reflect the real state of the network. Although GL is known for its capability to cope with single point failure, the inaccessible nodes will generate negative effect in the subsequent training rounds. On one hand, inaccessible nodes keep learning on its local data may deviate from accessible nodes and introduce bias. On the other hand, when the inaccessible nodes rejoin, the outdated local model integrated in the current gossip exchange will slow down the convergence.

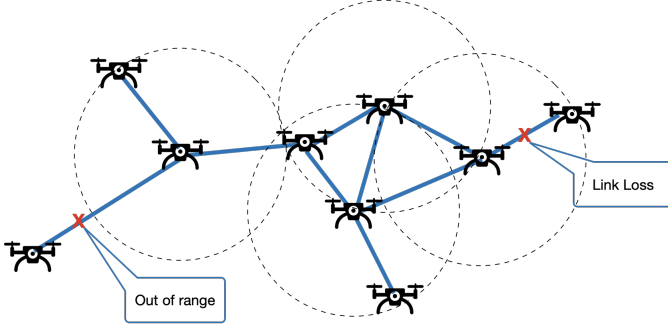


Fig. 1. The two scenarios that the average of all local models fails to reflect the GL state of the network.

Our work aims to formulate and investigate the impact of inaccessible nodes under dynamic network topology from the perspective of convergence analysis. To our best knowledge, this work offers the first theoretical investigation into the convergence of GL considering inaccessible nodes. Our contribution in this study are threefold.

- We find that the accessible and inaccessible nodes present different descent patterns. Furthermore, we find that the weight divergence between the average of all local models and average considering the inaccessibility is related to both data non-i.i.d.-ness and the number of inaccessible nodes.
- We investigate the GL convergence under the dynamic of node inaccessibility. Our findings show that the performance gap is an increasing function of inaccessible nodes and the inaccessible duration. The implications based on theoretical results are also provided.
- We conduct extensive numerical experiments to validate our findings, considering a comprehensive set of parameters, including the dropout rate, non-i.i.d.-ness across local data, and inaccessible duration from real agricultural UAV applications.

The paper is organized as follows. We present the related work in Section II. In Section III, we present the problem setup and assumptions. In Section IV, we provide the weight divergence, convergence analysis, and further practical implications. Numerical experiments are presented in Section V. Finally, we conclude the paper in Section VI.

Throughout this paper, we use the notation in Table I.

II. RELATED WORK

Gossip protocol [13] is an opportunistic protocol, and is originally designed to maintain consistency across a de-

TABLE I
NOTATION AND DEFINITIONS.

| Notation | Definitions |
|-------------------------------|--|
| $\ \cdot\ $ | ℓ_2 norm. |
| D_i, D | The data on the i -th node and the aggregation of all data, respectively. $D = \cup_{i=1}^n D_i$. |
| $\mathcal{S}, \mathcal{A}(t)$ | The set of all nodes and the set of accessible nodes at time t , respectively. Therefore, the set of inaccessible nodes is denoted by $\mathcal{S}/\mathcal{A}(t)$. |
| $\tau(t, i)$ | The number of inaccessible rounds of device i at time t . |
| $n_1(t), n_2(t), n$ | The number of nodes in $\mathcal{A}(t)$, $\mathcal{S}/\mathcal{A}(t)$, and \mathcal{S} respectively. $n = n_1(t) + n_2(t)$. |
| w_i, \bar{w}, \tilde{w} | The i -th local model, the average of all local models, and the average considering inaccessibility, respectively. |
| $F_i(\cdot), F(\cdot)$ | Local objective on the i -th node and global objective, respectively. |

centralized network, especially for a dynamic network, and to cope with single point failure. In particular, every node periodically sends out the new message to a subset of its neighbor nodes. Eventually, the entire network will receive the particular message with a high probability by the theory of random walk. Scholars in [14] extended it to gossip learning and applied it to decentralized linear models due to privacy considerations. Then, various learning schemes are explored, such as deep learning [15], reinforcement learning [16], and recommendation systems [17]. It was claimed in [6], [7] that GL can achieve similar or better performance compared to FL. There is another line working on the scalability [18] and efficiency [10]. To overcome the communication bottleneck, [10] proposed a gossip algorithm with compressed communication and analyzed convergence for unbiased and biased compression operators. Tang et al. proposed a sparsification algorithm [11], and Hashemi et al. focused on the impact of the number of gossip steps and studied the convergence for a non-convex objective [19]. Yuan et al. analyzed convergence of GL under convex objective and fixed learning rate [20]. However, since gossip protocol is an opportunistic protocol, all the aforementioned works studied the behavior of GL in terms of the average of all local models for convenience, which relies on the assumption that the gossip averaging preserves the average. However, in the presence of dropout nodes, this quantity does not represent the state of the whole network. The impacts of connectivity, data heterogeneity, number of dropout nodes, and dropout duration are still unclear. The understanding of the convergence behavior of GL is still in its infancy.

III. PROBLEM SETUP AND ASSUMPTIONS

A. Gossip Learning

Consider a scenario where n devices collaboratively train a model with parameter $w \in \mathbb{R}^d$. Each node i , $i \in [n]$ preserves a local model w_i and has its own data D_i . And we wish to minimize an objective function $F(w)$

$$F(w) := \frac{1}{n} \sum_{i=1}^n F_i(w), \quad (1)$$

where $F_i(\cdot)$ are the loss functions defined by the data available on each node.

Conventional FL training consists of local training and server aggregation steps. GL is the same as FL in the local training step, and the main difference lies in the aggregation step. Since the central server is absent in GL, the model sharing in GL is performed by a direct communication link between a pair of nodes, and we call such two nodes neighbors. The model aggregation is then performed in a self-organized way based on the connectivity of the network, in which the models are exchanged then average by each pair of neighboring nodes [10], [21]. GL is formally defined in [20].

- 1) **Gossiping average.** Each node i computes the weighted average by the gossiping matrix G , where its element $g_{ij} \neq 0$ only if j is a neighbor of i or $j = i$;

$$w_i^{t+\frac{1}{2}} = \sum_j g_{ij}^t w_j^t \quad (2)$$

- 2) **Local training.** Each node i updates its own local model w_i by running an Stochastic Gradient Descent (SGD) on the local dataset D_i and calculate the gradient:

$$\Delta w_i^{t+\frac{1}{2}} = \eta \nabla F_i(w_i^{t+\frac{1}{2}}), \quad (3)$$

where η is the learning rate, which can be either fixed or varying with t .

- 3) **Model update.** Each node applies the calculated gradients to the averaged model:

$$w_i^{(t+1)} = w_i^{t+\frac{1}{2}} - \Delta w_i^{t+\frac{1}{2}}. \quad (4)$$

Ideally, the nodes in the network are well-connected, and models can be averaged quickly and extensively. However, as we discussed, this does not depict a real-world scenario, especially in wireless and resource constrained case, in which a node may be out of range or experiencing a link loss. This motivates our evaluation of how node inaccessibility would affect the GL performance. We evaluate some basic questions regarding the node inaccessibility in GL: **(1) How much bias does the average of all local models introduce in the presence of inaccessible nodes? (2) How does number and duration of inaccessible nodes affect convergence of GL? (3) What variants may be potential to mitigate this bias?**

B. Assumptions and notation

This paper studies the convergence of GL under the following assumptions and notation.

Definition 1. (Gossip Matrix.) The gossip matrix $G = [g_{ij}] \in [0, 1]^{n \times n}$ associated with a connected graph satisfies: (1) If $i \neq j$ and i, j is not connected, then $g_{ij} = 0$; otherwise, $g_{ij} > 0$; (2) $G = G^T$ (symmetric); and (4) $\sum_i G_{ij} = \sum_j G_{ij} = 1$ (doubly stochastic).

Assumption 1. The loss functions $F_i(\cdot)$ for $i \in [n]$ are all L -smooth; that is, $\forall v, w \in \mathbb{R}^d$,

$$F_i(v) - F_i(w) \leq \langle v - w, \nabla F_i(w) \rangle + \frac{L}{2} \|v - w\|^2. \quad (5)$$

Assumption 2. The loss functions $F_i(\cdot)$ for $i \in [n]$ are all μ -strongly convex; that is, $\forall v, w \in \mathbb{R}^d$,

$$F_i(v) - F_i(w) \geq \langle v - w, \nabla F_i(w) \rangle + \frac{\mu}{2} \|v - w\|^2. \quad (6)$$

Assumption 3. The expectation of the squared ℓ_2 norm of the stochastic gradients is bounded; that is,

$$\mathbb{E}_\xi \|\nabla F_i(w, \xi)\|^2 \leq G^2, \quad (7)$$

where \mathbb{E}_ξ denotes the expectation against the randomness of the stochastic gradient.

Denote the optimal value for $F(\cdot)$ by F^* , and the optimal value for $F_i(\cdot)$ by F_i^* . Define Γ as a measurement of non-i.i.d.-ness across clients: $\Gamma \triangleq \sum_{i=1}^n \frac{n_i}{n} F_i^* - F^*$, where $\Gamma \geq 0$ indicates how non-i.i.d. across the client's data. Note that given a large enough number of data samples on nodes, we have $\Gamma \rightarrow 0$ for i.i.d. data distributions. We use notation w_i^t to denote the model on node i at time t .

IV. CONVERGENCE ANALYSIS

Each node in GL may present different learning patterns due to network connectivity, data heterogeneity among nodes, the number of SGD performed on each nodes, the number of gossip steps, and etc. In the presence of inaccessible nodes, the descent on such nodes does not contribute to the descent of \bar{w} , therefore simply taking average of all local models leads to biased error in the convergence analysis. In addition, in FL, the outdated models of dropout nodes are overwritten by the latest models before rejoining training. In contrast, GL retains and merges the outdated models once they become accessible again. As a result, dropped nodes not only stall the convergence but also introduce bias to the learned model. Therefore, it is necessary to study the behavior of accessible and inaccessible nodes separately.

A. Weight Divergence

Instead of ignoring inaccessible nodes in other works, we classify the nodes into accessible nodes and inaccessible nodes by whether they successfully transmit the model to their neighbors or not. To jointly describe both type of nodes, we define the average with inaccessibility, which is illustrated in Fig. 2.

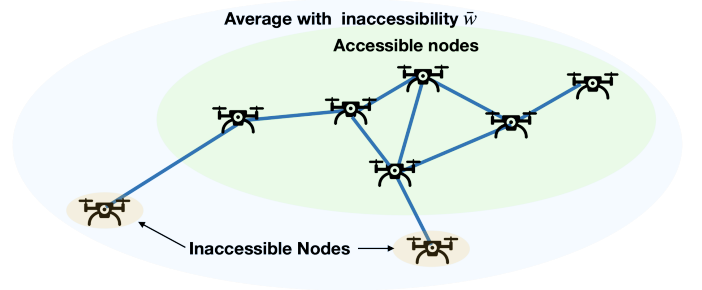


Fig. 2. Illustration of average with inaccessibility.

Definition 2. (Average with inaccessibility.) Define the set of accessible nodes at time t as $\mathcal{A}(t)$. For each $i \in \mathcal{A}(t)$, $g_{ii} \neq 1$.

And the remaining nodes $i \in \mathcal{S}/\mathcal{A}(t)$ are dropped out due to link loss or out of range. Denote the cardinality of $\mathcal{A}(t)$ and $\mathcal{S}/\mathcal{A}(t)$ by $n_1(t)$ and $n_2(t)$, respectively. The average with inaccessible nodes is defined as

$$\bar{w}^t := \frac{1}{n_1(t)} \sum_{i,j \in \mathcal{A}(t)} w_i^t + \frac{1}{n_2(t)} \sum_{i \in \mathcal{S}/\mathcal{A}(t)} w_i^t. \quad (8)$$

The average of all local models are denoted as: $\bar{w} = \frac{1}{n} \sum_{i \in \mathcal{S}} w_i$. The gradient of two averages shows different patterns:

$$g(\bar{w}^t) = \nabla F_i(\bar{w}^t), \quad (9)$$

$$g(\bar{w}^t) = \frac{n_1(t)}{n} \nabla F_i\left(\frac{1}{n_1(t)} \sum_{i \in \mathcal{A}(t)} w_i^t\right) + \frac{1}{n} \sum_{i \in \mathcal{S}/\mathcal{A}(t)} \nabla F_i(w_i^t). \quad (10)$$

$g(\bar{w}^t)$ in Eq. 6 is simply the gradient on the average of all local models, while $g(\bar{w}^t)$ in Eq. 7 is a weight average of the gradient of the average of all accessible nodes, $\nabla F_i(\frac{1}{n_1(t)} \sum_{i \in \mathcal{A}(t)} w_i^t)$, and the average gradient of inaccessible models, $\frac{1}{n} \sum_{i \in \mathcal{S}/\mathcal{A}(t)} \nabla F_i(w_i^t)$. The descent of the average of all local models, the average of accessible nodes, and inaccessible nodes presents different patterns and can be visualized in Fig. 3. When all nodes are connected (red line), the average is preserved and the local models become more similar after gossip average, thus enjoys the best convergence. However, in the presence of inaccessible nodes, the average on accessible nodes only introduces bias (blue line). In addition, inaccessible nodes training the local model on their own data would also introduce divergence (green lines). We give the formal expression of the weight divergence in the following proposition.

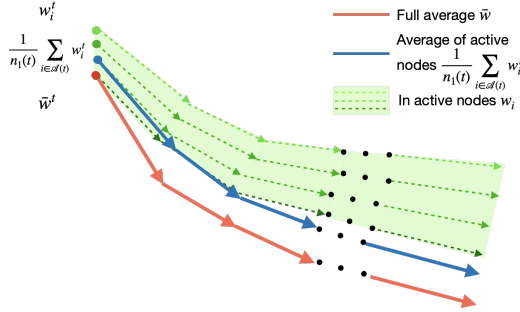


Fig. 3. Illustration of the weight divergence of full consensus model \bar{w} , partial consensus model \tilde{w} and individual models w_i .

Proposition 1. If F_i is L -smooth, then we have the following inequality for the weight divergence of between the gradient of the average of all local models \bar{w} and the gradient of average with inaccessibility \tilde{w} :

$$\begin{aligned} & \|g(\bar{w}^{t+1}) - g(\tilde{w}^{t+1})\| \\ & \leq \frac{L\eta^2}{n} \left[\underbrace{n_1(t) \left\| \frac{1}{n_1(t)} \sum_{i,j \in \mathcal{A}(t)} w_i^t - \bar{w}^t \right\|}_{\text{accessible nodes}} + \underbrace{\sum_{i \in \mathcal{S}/\mathcal{A}(t)} \|w_i^t - \bar{w}^t\|}_{\text{inaccessible nodes}} \right] \end{aligned} \quad (11)$$

The proof can be found in Appendix A.

Remark 1. The first term comes from the accessible nodes, and can be seen as the difference between the sample mean and population mean. Increasing the number of accessible nodes will decrease the first term. The second term comes from the inaccessible nodes, and longer inaccessible duration and larger internal training rounds will increase the second term.

B. Convergence under Node Inaccessibility

To further analyze the iterative effect of node inaccessibility, we adopt the definition from [22] to quantify the dynamics of inaccessible nodes.

Definition 3. Number of inaccessible rounds. The inaccessible duration of node i at time t is defined as $\tau(t, i) = t - \max t' | t' \leq t, i \in \mathcal{A}(t')$, which is the difference between the current time t and the last time that node i is accessible.

For convenience, we assume the inaccessible duration follows an exponential distribution, i.e., $\tau(t, i) \sim \exp(\lambda)$, and we have $\mathbb{E}[\tau(t, i)] = \frac{1}{\lambda}$.

Theorem 1. If the objective function F_i is strongly convex and L -smooth, and has bounded gradient, GL satisfies

$$\mathbb{E}[\|\bar{w}^{t+1} - w^*\|^2] \leq \alpha(t)^t \mathbb{E}[\|\bar{w}^0 - w^*\|^2] + \sum_{i=0}^{t-1} \alpha(t)^i \beta(t) \quad (12a)$$

$$\alpha(t) = 2(1 - \mu\eta) \quad (12b)$$

$$\begin{aligned} \beta(t) = & \frac{1}{n} [\eta L n_1(t) \left\| \frac{1}{n_2(t)} \sum_{i \in \mathcal{S}/\mathcal{A}(t)} w_i^t \right\|^2 + 4\eta\Gamma + 2n_1(t)\eta^2 G^2 \\ & + 2n_2(t)G^2(2\eta^3(1 + \frac{1}{\lambda}) + \frac{2\mu(1-\eta)}{\lambda})] \end{aligned} \quad (12c)$$

The proof can be found in Appendix B.

Remark 2. We remark that $\beta(t)$ is an increasing function of the difference between the average of local models of accessible nodes and the average of all local models, i.e., $\left\| \frac{1}{n_2(t)} \sum_{i \in \mathcal{S}/\mathcal{A}(t)} w_i^t \right\|^2$, indicating the different in last iteration is inherited. In addition, $\beta(t)$ is a decreasing function of λ . Therefore, longer inaccessibility will slow down the convergence. Finally, we note that the data heterogeneity still plays an important role in the convergence of GL, as the same as in FL.

Remark 3. The term, $\frac{4\mu n_2(t)G^2}{\lambda}$, in $\beta(t)$ is not scaled by the learning rate η . Therefore, even for a decreasing learning rate, where $\lim_{t \rightarrow \infty} \eta(t) = 0$, we have $\lim_{t \rightarrow \infty} \beta(t) \neq 0$. We highlight that in the presence of node inaccessibility, GL does not converge to its optimal.

C. Practical Implications

Our findings deliver significant practical implications.

1) *Increase the Number of Accessible Nodes.* $\frac{1}{n_1(t)} \sum_{i \in \mathcal{A}(t)} w_i^t$ can be treated as the sample mean that drawn from w_i^t , while \bar{w} can be seen as the population mean. The difference $\left\| \frac{1}{n_1(t)} \sum_{i \in \mathcal{A}(t)} w_i^t - \bar{w}^t \right\|$ is related to the variance of local models, which is originated from

data heterogeneity and the sample size, $n_1(t)$. Improving connectivity can reduce this difference. Our findings also explain why “critical consensus distance” in [23] is a factor of convergence.

2) *Reduce Data Heterogeneity*: According to Eq. 10, the data heterogeneity affects GL by the gradient of gossiping averaged model descent on the local data, i.e., $\nabla F_i(\bar{w}, D_i)$, and inaccessible nodes train on their local data individually, i.e., $\nabla F_i(w_i, D_i)$. More non-i.i.d. local distributions among nodes will result in higher divergence in both terms. Applying drift correction can help preserve distributional stability after averaging. In addition, following the intuition that some data are more critical than others. It is beneficial to train on those nodes more frequently.

3) *De-emphasize the model update of inaccessible nodes when they rejoin*: We also notice that the longer the node stays inaccessible, the greater the weight divergence. To mitigate the weight divergence of inaccessible nodes that are back online, one could de-emphasize the outdated model in the averaging operation.

V. NUMERICAL EXPERIMENTS

A. Experimental Setup

1) *Datasets and Models*: Model architecture ResNet-18 [24] is employed in our experiments. Models are trained on CIFAR-10 dataset [25]. The dataset contains 60,000 32×32 color images across 10 classes, with each class containing 5,000 training images and 1,000 test images.

2) *Training setting*: We report the training parameters in Tab. III. We further introduce two data heterogeneity settings. The first one is *i.i.d. assignment*, in which each node is assigned 6000/100, and the data distribution on each node is the same as the distribution of the whole dataset. The second one is *non-i.i.d. assignment*, in which nodes do not have equal amount of data and the data distribution on each node is different from the whole dataset. We use Dirichlet distribution with a hyper-parameter $\alpha \in \{1, 10\}$ to generate different data distributions for users, where a smaller α indicates a greater non-i.i.d.-ness. The i.i.d. setting provides the performance upper bound, while the non-i.i.d. setting represents practical scenarios, providing us the insight of how non-i.i.d.-ness downgrades the performance in real applications.

TABLE II
HYPER-TRAINING PARAMETERS

| Epoch | Nodes | Batch size | Learning rate | Local epochs |
|-------|-------|------------|---------------|--------------|
| 50 | 14 | 128 | 0.1 | 2 |

3) *Node Movement Simulation*: To simulate the device movement in a dynamic network, we use the Random Way-point model [26]. Each node holds their own dataset D_i and local model w_i . The operation area is $1000m \times 1000m$. The trajectories of nodes are generated by the following steps:

- i) The node i assumes an initial location (x_i^0, y_i^0) .
- ii) Each node moves randomly with a speed v_i chosen uniformly from an interval $[5m/s, 7m/s]$.

- iii) The node pauses 1 s for t_i after reaching (x_i, y_i) .
- iv) $i = i + 1$ and go to step ii).

The communication radius to $r = 250m$. We further set the probability that a node fails to communicate to its neighbors to $p \in \{0\%, 10\%, 20\%\}$. When a node becomes inaccessible, the duration of inaccessibility is drawn from an exponential distribution with parameter $\lambda \in \{0.2, 0.3, 0.5\}$. That is, the node being inaccessible at time t will rejoin training at time $t + \exp(\lambda)$. And larger λ indicates shorter inaccessible duration. The connectivity of out-of-range and inaccessible nodes is set to 0, and 1 otherwise. Finally, the connectivity matrix is transformed into a doubly matrix.

4) *Implementations*: All our experiments are conducted on a computing cluster with NVIDIA A100 Tensor Core GPU @ 40 GB and Intel Xeon Gold 6138 CPU @ 2.00 GHz. Node movements are generated by ns-3. The learning process is implemented based on PyTorch.

B. Results

We plot the average local test accuracy and sum of training loss as a function of training epoch in Fig. 4, considering dropout rate p , data non-i.i.d.-ness α , and offline duration parameter λ . The final accuracy and number of inaccessible nodes for each setting are summarized in Table V-B. In the first column of Fig. 4, we consider the dropout rate $p \in \{0\%, 10\%, 20\%\}$. We fixed other two factors to be $\alpha = 10$ and $\lambda = 1$. At the beginning, the three curves exhibit identical convergence rates, which is in line with the convergence rate term $\alpha(t)$ in Theorem 1. As for the final model accuracy, the non-dropout setting yields the best result, while dropout settings suffer slight performance drops, which differs from the established knowledge that GL is robust against the node dropouts. Moreover, a slight drop in accuracy is observed in dropout settings after the convergence is reached. One possible explanation is that the frequent changes in participating nodes have an impact on the stability of the convergence.

In the second column of Fig. 4, we present the convergence performance of under data non-i.i.d.-ness, represented by $\alpha \in 1, 10, \infty$, with ∞ indicating the data is i.i.d.. The i.i.d. setting results in the best convergence, while greater non-i.i.d.-ness leads to reduced accuracy. We can also see that the impact of data non-i.i.d.-ness outweighs the other factors, highlighting that the data heterogeneity remains a big challenge in GL.

In the third column, we investigate the $\lambda \in \{0.2, 0.3, 0.5\}$. In the dropout rate settings, we examine the the impact of multiple node dropouts in one training epoch. In contrast, the λ reflects the lagging effect of one node dropout for multiple training epochs. Smaller λ indicating a longer inaccessible duration results in a larger performance drop. It can also be seen that the accuracy of the non-dropout case is stable while other three curves experience more fluctuations.

VI. CONCLUSION

In this paper, we have investigated the impact of inaccessible nodes under dynamic network topology. We have proved that the number of inaccessible nodes, data non-i.i.d.-ness, and

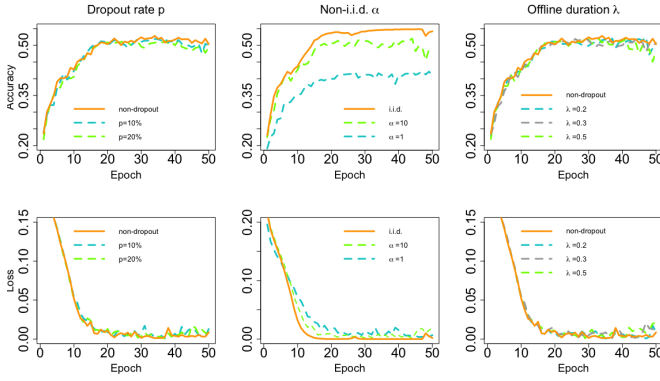


Fig. 4. The mean test accuracy (first row) and sum of training loss (second row) under different p , α , λ .

TABLE III
AVERAGE MODEL ACCURACY

| Non-i.i.d. α | Dropout rate p | Duration λ | Inaccessible nodes | Accuracy (%) |
|---------------------|------------------|--------------------|--------------------|------------------|
| 10 | 0% | 1 | 1.30 ± 0.81 | 52.82 ± 5.45 |
| | 10% | | 3.52 ± 1.76 | 49.88 ± 5.66 |
| | 20% | | 5.54 ± 1.87 | 48.31 ± 6.18 |
| ∞ | 5% | 1 | | 54.18 ± 3.87 |
| 10 | | | 2.37 ± 1.48 | 49.38 ± 7.72 |
| 1 | | | | 42.28 ± 6.62 |
| 10 | 10% | 0.2 | 7.26 ± 2.58 | 50.71 ± 8.04 |
| | | 0.33 | 5.56 ± 2.27 | 50.53 ± 6.58 |
| | | 0.5 | 4.60 ± 2.07 | 48.85 ± 7.04 |

duration of inaccessibility negatively affect the GL convergence. Further more, we have also proved that the GL does not converge to the optimum in the presence of inaccessible nodes. The convergence gap in the presence of node inaccessibility can be reduced by improving network connectivity, applying bias correction and node selection algorithms, and de-emphasize the model of inaccessible nodes when they re-join training. Extensive experiments conducted under practical conditions verified the correctness of our findings.

REFERENCES

- [1] C. Qu, J. Boubin, D. Gafurov, J. Zhou, N. Aloysius, H. Nguyen, and P. Calyam, "Uav swarms in smart agriculture: Experiences and opportunities," in *2022 IEEE 18th International Conference on e-Science (e-Science)*. IEEE, 2022, pp. 148–158.
- [2] D. Albani, T. Manoni, A. Arik, D. Nardi, and V. Trianni, "Field coverage for weed mapping: toward experiments with a uav swarm," in *Bio-inspired Information and Communication Technologies: 11th EAI International Conference, BICT 2019, Pittsburgh, PA, USA, March 13–14, 2019, Proceedings 11*. Springer, 2019, pp. 132–146.
- [3] S. Yu, J. Zhu, J. Zhou, J. Cheng, X. Bian, J. Shen, and P. Wang, "Key technology progress of plant-protection uavs applied to mountain orchards: A review," *Agronomy*, vol. 12, no. 11, p. 2828, 2022.
- [4] A. Davis, P. S. Wills, J. E. Garvey, W. Fairman, M. A. Karim, and B. Ouyang, "Developing and field testing path planning for robotic aquaculture water quality monitoring," *Applied Sciences*, vol. 13, no. 5, p. 2805, 2023.
- [5] M. Mohan, G. Richardson, G. Gopan, M. M. Aghai, S. Bajaj, G. P. Galgamuwa, M. Vastaranta, P. S. P. Arachchige, L. Amorós, A. P. D. Corte *et al.*, "Uav-supported forest regeneration: Current trends, challenges and implications," *Remote Sensing*, vol. 13, no. 13, p. 2596, 2021.
- [6] I. Hegedűs, G. Danner, and M. Jelasity, "Gossip learning as a decentralized alternative to federated learning," in *Distributed Applications and Interoperable Systems: 19th IFIP WG 6.1 International Conference,*

- DAIS 2019, Held as Part of the 14th International Federated Conference on Distributed Computing Techniques, DisCoTec 2019, Kongens Lyngby, Denmark, June 17–21, 2019, Proceedings 19*. Springer, 2019, pp. 74–90.
- [7] I. Hegedűs, G. Danner, and M. Jelasity, "Decentralized learning works: An empirical comparison of gossip learning and federated learning," *Journal of Parallel and Distributed Computing*, vol. 148, pp. 109–124, 2021.
- [8] X. Lian, C. Zhang, H. Zhang, C.-J. Hsieh, W. Zhang, and J. Liu, "Can decentralized algorithms outperform centralized algorithms? a case study for decentralized parallel stochastic gradient descent," *Advances in neural information processing systems*, vol. 30, 2017.
- [9] L. Giaretta and Š. Girdzijauskas, "Gossip learning: Off the beaten path," in *2019 IEEE International Conference on Big Data (Big Data)*. IEEE, 2019, pp. 1117–1124.
- [10] A. Koloskova, S. Stich, and M. Jaggi, "Decentralized stochastic optimization and gossip algorithms with compressed communication," in *International Conference on Machine Learning*. PMLR, 2019, pp. 3478–3487.
- [11] Z. Tang, S. Shi, B. Li, and X. Chu, "Gossipfl: A decentralized federated learning framework with sparsified and adaptive communication," *IEEE Transactions on Parallel and Distributed Systems*, vol. 34, no. 3, pp. 909–922, 2022.
- [12] A. Hashemi, A. Acharya, R. Das, H. Vikalo, S. Sanghavi, and I. Dhillon, "On the benefits of multiple gossip steps in communication-constrained decentralized federated learning," *IEEE Transactions on Parallel and Distributed Systems*, vol. 33, no. 11, pp. 2727–2739, 2021.
- [13] S. Boyd, A. Ghosh, B. Prabhakar, and D. Shah, "Randomized gossip algorithms," *IEEE transactions on information theory*, vol. 52, no. 6, pp. 2508–2530, 2006.
- [14] R. Ormándi, I. Hegedűs, and M. Jelasity, "Gossip learning with linear models on fully distributed data," *Concurrency and Computation: Practice and Experience*, vol. 25, no. 4, pp. 556–571, 2013.
- [15] M. Blot, D. Picard, M. Cord, and N. Thome, "Gossip training for deep learning," *arXiv preprint arXiv:1611.09726*, 2016.
- [16] A. Mathkar and V. S. Borkar, "Distributed reinforcement learning via gossip," *IEEE Transactions on Automatic Control*, vol. 62, no. 3, pp. 1465–1470, 2016.
- [17] Y. Belal, A. Bellet, S. B. Mokhtar, and V. Nitu, "Pepper: Empowering user-centric recommender systems over gossip learning," *Proceedings of the ACM on Interactive, Mobile, Wearable and Ubiquitous Technologies*, vol. 6, no. 3, pp. 1–27, 2022.
- [18] J. Daily, A. Vishnu, C. Siegel, T. Warfel, and V. Amaty, "Gossipgrad: Scalable deep learning using gossip communication based asynchronous gradient descent," *arXiv preprint arXiv:1803.05880*, 2018.
- [19] A. Hashemi, A. Acharya, R. Das, H. Vikalo, S. Sanghavi, and I. Dhillon, "On the benefits of multiple gossip steps in communication-constrained decentralized federated learning," *IEEE Transactions on Parallel and Distributed Systems*, vol. 33, no. 11, pp. 2727–2739, 2022.
- [20] K. Yuan, Q. Ling, and W. Yin, "On the convergence of decentralized gradient descent," *SIAM Journal on Optimization*, vol. 26, no. 3, pp. 1835–1854, 2016.
- [21] J. Chen, S. Wang, L. Carin, and C. Tao, "Finite-time consensus learning for decentralized optimization with nonlinear gossiping," *arXiv preprint arXiv:2111.02949*, 2021.
- [22] X. Gu, K. Huang, J. Zhang, and L. Huang, "Fast federated learning in the presence of arbitrary device unavailability," *Advances in Neural Information Processing Systems*, vol. 34, pp. 12 052–12 064, 2021.
- [23] T. Zhu, F. He, L. Zhang, Z. Niu, M. Song, and D. Tao, "Topology-aware generalization of decentralized sgd," in *International Conference on Machine Learning*. PMLR, 2022, pp. 27 479–27 503.
- [24] K. He, X. Zhang, S. Ren, and J. Sun, "Identity mappings in deep residual networks," in *Computer Vision—ECCV 2016: 14th European Conference, Amsterdam, The Netherlands, October 11–14, 2016, Proceedings, Part IV 14*. Springer, 2016, pp. 630–645.
- [25] A. Krizhevsky, G. Hinton *et al.*, "Learning multiple layers of features from tiny images," 2009.
- [26] S. Mao, "Chapter 8 - fundamentals of communication networks," in *Cognitive Radio Communications and Networks*, A. M. Wyglinski, M. Nekovee, and Y. T. Hou, Eds. Oxford: Academic Press, 2010, pp. 201–234. [Online]. Available: <https://www.sciencedirect.com/science/article/pii/B9780123747150000083>

APPENDIX

A. Proof of Proposition 1

Proof. At the t -th training rounds, the gradient of \bar{w} and \tilde{w} are:

$$g(\bar{w}^t) = \nabla F_i(\bar{w}^t)$$

$$g(\tilde{w}^t) = \frac{n_1(t)}{n} \nabla F_i\left(\frac{1}{n_1(t)} \sum_{i \in \mathcal{A}(t)} w_i^t\right) + \frac{1}{n} \sum_{i \in S/\mathcal{A}(t)} \nabla F_i(w_i^t),$$

By assumption 2, we have

$$\begin{aligned} & \|g(\tilde{w}^{t+1}) - g(\bar{w}^{t+1})\| \\ & \leq \frac{n_1(t)}{n} \left[\left\| \frac{1}{n_1(t)} \sum_{i \in \mathcal{A}(t)} w_i^t - \bar{w}^t \right\| + \eta \left\| \nabla F_i\left(\frac{1}{n_1(t)} \sum_{i \in \mathcal{A}(t)} w_i^t\right) - \nabla F_i(\bar{w}^t) \right\| \right] + \frac{n_2(t)}{n} \left[\sum_{i \in S/\mathcal{A}(t)} \|w_i^t - \bar{w}^t\| + \eta \left\| \sum_{i \in S/\mathcal{A}(t)} (\nabla F_i(w_i^t) - \nabla F_i(\bar{w}^t)) \right\| \right] \\ & \stackrel{(a)}{\leq} \frac{1 + L\eta^2}{n} \left[n_1(t) \left(\left\| \sum_{i \in \mathcal{A}(t)} w_i^t - w^t \right\| + \sum_{i \in S/\mathcal{A}(t)} \|w_i^t - w^t\| \right) \right], \end{aligned} \quad (13)$$

□

where (a) is due to Assumption 1.

B. Proof of Theorem 1

Proof.

$$\begin{aligned} & \|\tilde{w}^{t+1} - w^*\|^2 \\ & \leq \left\| \frac{n_1(t)}{n} [\tilde{w} - \nabla F_i\left(\frac{1}{n_1(t)} \sum_{i \in \mathcal{A}(t)} w_i^t\right) - w^*] + \frac{1}{n} \sum_{i \in S/\mathcal{A}(t)} [w_i^t - \nabla F_i(w_i^t) - w^*] \right\|^2 \\ & \stackrel{(b)}{\leq} 2\|\tilde{w}^t - w^*\|^2 - \underbrace{\frac{n_1(t)}{n} [4\eta \langle \nabla F_i\left(\frac{1}{n_1(t)} \sum_{i \in \mathcal{A}(t)} w_i^t\right), \tilde{w}^t - w^* \rangle + 2\eta^2 \|\nabla F_i\left(\frac{1}{n_1(t)} \sum_{i \in \mathcal{A}(t)} w_i^t\right)\|^2]}_{A_1} \\ & \quad - \underbrace{\frac{1}{n} [4\eta \sum_{i \in S/\mathcal{A}(t)} \langle \nabla F_i(w_i^t), \tilde{w}^t - w^* \rangle + 2\eta^2 \sum_{i \in S/\mathcal{A}(t)} \|\nabla F_i(w_i^t)\|^2]}_{A_2}, \end{aligned} \quad (14)$$

where (b) is due to $\|a + b\| \leq 2\|a\| + 2\|b\|$.

$$\begin{aligned} -A_1 &= -4\eta \left[\left\langle \tilde{w}^t - \frac{1}{n_1(t)} \sum_{i \in \mathcal{A}(t)} w_i^t + \frac{1}{n_1(t)} \sum_{i \in \mathcal{A}(t)} w_i^t - w^*, \nabla F_i\left(\frac{1}{n_1(t)} \sum_{i \in \mathcal{A}(t)} w_i^t\right) \right\rangle \right] \\ &= -4\eta \left[\left\langle \tilde{w}^t - \frac{1}{n_1(t)} \sum_{i \in \mathcal{A}(t)} w_i^t, \nabla F_i\left(\frac{1}{n_1(t)} \sum_{i \in \mathcal{A}(t)} w_i^t\right) \right\rangle + \left\langle \frac{1}{n_1(t)} \sum_{i \in \mathcal{A}(t)} w_i^t - w^*, \nabla F_i\left(\frac{1}{n_1(t)} \sum_{i \in \mathcal{A}(t)} w_i^t\right) \right\rangle \right] \\ &\stackrel{(c)}{\leq} -4\eta [F_i(\tilde{w}^t) - F_i\left(\frac{1}{n_1(t)} \sum_{i \in \mathcal{A}(t)} w_i^t\right) - \frac{L}{2} \|\tilde{w}^t - \frac{1}{n_1(t)} \sum_{i \in \mathcal{A}(t)} w_i^t\|^2 + F_i\left(\frac{1}{n_1(t)} \sum_{i \in \mathcal{A}(t)} w_i^t\right) - F_i(w^*) + \frac{\mu}{2} \|\frac{1}{n_1(t)} \sum_{i \in \mathcal{A}(t)} w_i^t - w^*\|^2] \\ &\leq -4\eta [F_i(\tilde{w}^t) - F_i(w^*)] + 2L\eta \|\tilde{w}^t - \frac{1}{n_1(t)} \sum_{i \in \mathcal{A}(t)} w_i^t\|^2 - 2\mu\eta \sum_{i \in \mathcal{A}(t)} \|w_i^t - w^*\|^2 \\ &\leq -4\eta L \|\tilde{w}^t - w^*\|^2 + 2L\eta \|\tilde{w}^t - \frac{1}{n_1(t)} \sum_{i \in \mathcal{A}(t)} w_i^t\|^2 - 2\mu\eta \sum_{i \in \mathcal{A}(t)} \|w_i^t - w^*\|^2 \end{aligned} \quad (15)$$

where (c) is due to Assumptions 1 and 2.

$$\begin{aligned} -A_2 &= \frac{4\eta}{n} \sum_{i \in S/\mathcal{A}(t)} \langle w^* - \tilde{w}^t + w_i^{t-\tau(t,i)} - w_i^{t-\tau(t,i)}, \nabla F_i(w_i^{t-\tau(t,i)}) \rangle \\ &= \underbrace{\frac{4\eta}{n} \sum_{i \in S/\mathcal{A}(t)} \langle w_i^{t-\tau(t,i)} - w^t, \nabla F_i(w_i^{t-\tau(t,i)}) \rangle}_{B_1} - \underbrace{\frac{4\eta}{n} \sum_{i \in S/\mathcal{A}(t)} \langle w_i^{t-\tau(t,i)} - w^*, \nabla F_i(w_i^{t-\tau(t,i)}) \rangle}_{B_2} \end{aligned} \quad (16)$$

$$\begin{aligned}
B_1 &\leq \frac{4\eta}{n} \sum_{i \in \mathcal{S}/\mathcal{A}(t)} \|w_i^{t-\tau(t,i)} - w^t\|^2 + \frac{4\eta^3}{n} \sum_{i \in \mathcal{S}/\mathcal{A}(t)} \|\nabla F_i(w_i^{t-\tau(t,i)})\|^2 \\
&\leq \frac{4\eta^3 n_2(t)}{n\lambda} \|\nabla F_i(w_i^{t-\tau(t,i)})\|^2 + \frac{4\eta^3 n_2(t)}{n} \|\nabla F_i(w_i^{t-\tau(t,i)})\|^2 \\
&\stackrel{(d)}{\leq} \frac{4\eta^3 n_2(t)}{n} (1 + \frac{1}{\lambda}) G^2
\end{aligned} \tag{17}$$

In the last inequality (d), we assume the inaccessible duration follows an exponential distribution, i.e., $\tau(t, i) \sim \exp(\lambda)$, and we have $\mathbb{E}[\tau(t, i)] = \frac{1}{\lambda}$.

$$\begin{aligned}
-B_2 &\leq \frac{4\eta}{n} \sum_{i \in \mathcal{S}/\mathcal{A}(t)} [\langle w^* - w_i^{t-\tau(t,i)}, \nabla F_i(w_i^{t-\tau(t,i)}) \rangle] \\
&\stackrel{(e)}{\leq} \frac{4\eta}{n} \sum_{i \in \mathcal{S}/\mathcal{A}(t)} [F_i(w^*) - F_i(w_i^{t-\tau(t,i)}) - \frac{\mu}{2} \|w_i^{t-\tau(t,i)} - w^*\|^2] \\
&\leq \frac{4\eta}{n} \sum_{i \in \mathcal{S}/\mathcal{A}(t)} [F_i(w^*) - F_i^* + F_i^* - F_i(w_i^{t-\tau(t,i)}) - \frac{\mu}{2} \|w_i^{t-\tau(t,i)} - w^*\|^2] \\
&= \frac{4\eta}{n} \sum_{i \in \mathcal{S}/\mathcal{A}(t)} (F_i(w^*) - F_i^*) + \frac{4\eta}{n} \sum_{i \in \mathcal{S}/\mathcal{A}(t)} (F_i^* - F_i(w_i^{t-\tau(t,i)})) - \frac{2\mu\eta}{n} \sum_{i \in \mathcal{S}/\mathcal{A}(t)} [\|w_i^{t-\tau(t,i)} - w^*\|^2] \\
&\stackrel{(f)}{\leq} \frac{4\eta n_2(t)}{n} \Gamma - \frac{2\mu\eta}{n} \sum_{i \in \mathcal{S}/\mathcal{A}(t)} \underbrace{[\|w_i^{t-\tau(t,i)} - w^*\|^2]}_C,
\end{aligned} \tag{18}$$

where (e) is due to Assumptions 2, and (f) is by the definition of Γ and the fact that $(F_i^* - F_i(w_i)) \leq 0$

$$\begin{aligned}
-C &\leq -\|w_i^{t-\tau(t,i)} - w_i^t\|^2 - \|w_i^t - w^*\|^2 - 2\langle w_i^{t-\tau(t,i)} - w^t, w^t - w^* \rangle \\
&\leq -\|w_i^{t-\tau(t,i)} - w_i^t\|^2 - \|w_i^t - w^*\|^2 + \frac{1}{\eta} \|w_i^{t-\tau(t,i)} - w^t\|^2 + \eta \|w_i^t - w^*\|^2 \\
&= -(1 - \eta) \|w_i^t - w^*\|^2 + (\frac{1}{\eta} - 1) \|w_i^{t-\tau(t,i)} - w_i^t\|^2 \\
&\leq -(1 - \eta) \left[\frac{G^2}{\eta\lambda} - \|w_i^t - w^*\|^2 \right]
\end{aligned} \tag{19}$$

This completes the proof. \square